Targeted viral vector transduction of relaxin-3 neurons in the rat *nucleus incertus* using a novel cell-type specific promoter

Alexander D. Wykes[a,b], Sherie Ma[a,b,1], Ross A.D. Bathgate[a,b,c,]*, Andrew L. Gundlach[a,b,]*

[a] *The Florey Institute of Neuroscience and Mental Health, The University of Melbourne, Victoria, Australia*
[b] *Florey Department of Neuroscience and Mental Health, The University of Melbourne, Victoria, Australia*
[c] *Department of Biochemistry and Molecular Biology, The University of Melbourne, Victoria, Australia*

ABSTRACT

Modern neuroscience utilizes transgenic techniques extensively to study the activity and function of brain neural networks. A key feature of this approach is its compatibility with molecular methods for selective transgene expression in neuronal circuits of interest. Until now, such targeted transgenic approaches have not been applied to the extensive circuitry involving the neuropeptide, relaxin-3. Pharmacological and gene knock-out studies have revealed relaxin-3 signalling modulates interrelated behaviours and cognitive processes, including stress and anxiety, food and alcohol consumption, and spatial and social memory, highlighting the potential of this system as a therapeutic target. In the present study, we aimed to identify a promoter sequence capable of regulating cell-type specific transgene expression from an adeno-associated viral (AAV) vector in relaxin-3 neurons of the rat *nucleus incertus* (NI). In parallel to relaxin-3 promoter sequences, we also tested an AAV vector containing promoter elements for the tropomyosin receptor kinase A (TrkA) gene, as TrkA is co-expressed with relaxin-3 in rat NI neurons. Stereotaxic injection of an mCherry-expressing AAV vector revealed widespread non-specific TrkA promoter (880 bp) activity in and adjacent to the NI at 8 weeks post-treatment. In contrast, mCherry expression was successfully restricted to relaxin-3 NI neurons with 98% specificity using a 1736 bp relaxin-3 promoter. In addition to detailed anatomical mapping of NI relaxin-3 networks, illustrated here in association with GABAergic medial septum neurons, this method for targeted transgene delivery offers a versatile tool for ongoing preclinical studies of relaxin-3 circuitry.

Introduction

States of wakefulness, which broadly influence behaviour and cognitive function, are maintained by basal forebrain, hypothalamic, thalamic and brainstem neurons via a range of chemical and peptide transmitters (Jones, 2003). Among these, the neuropeptide, relaxin-3, has emerged as a highly-conserved modulator of arousal in vertebrate species. While primarily located within the brainstem *nucleus incertus* (NI) (Burazin et al., 2002), relaxin-3 neurons are also found in the periaqueductal grey (PAG), pontine raphe nucleus and a region dorsal to the substantia nigra in rat (Tanaka et al., 2005), mouse (Smith et al., 2010) and macaque (Ma et al., 2009b) brain. The vast majority of NI neurons produce γ-aminobutyric acid (GABA), with around one-third of GABAergic NI neurons expressing relaxin-3 (Ma et al., 2007, 2017a). Various other neuropeptides, including cholecystokinin (Kubota et al., 1983; Olucha-Bordonau et al., 2003) and neuromedin B (Chronwall et al., 1985), along with the calcium-binding proteins, calbindin and calretinin (Paxinos et al., 1999; Ma et al., 2007), are also expressed in the NI, indicating a specialised role for relaxin-3 neurons amongst these heterogenous populations.

The anatomical location and innervation pattern of the NI (Goto et al., 2001; Olucha-Bordonau et al., 2003) suggest relaxin-3 signalling from this nucleus is driven by integrated inputs related to behavioural planning, and in turn, modulates appropriate cognitive activity and responses. For example, blockade of corticotropin-releasing factor-1 (CRF_1) (Walker et al., 2017) or orexin-2 (OX_2) (Kastman et al., 2016) receptors attenuates stress-induced relapse to alcohol-seeking in alcohol-preferring (iP) rats, with NI relaxin-3 neurons expressing receptors for, and being responsive to, these peptides (Ma et al., 2013; Blasiak et al., 2015). 5-HT_{1A} serotonin (Miyamoto et al., 2008) and D_2 dopamine (Kumar et al., 2015) receptors are also expressed by relaxin-3 NI neurons, and have been implicated in anxiety (Kumar et al., 2016)

and locomotor (Kumar et al., 2015) behaviour, respectively. These various integrated inputs are conveyed by ascending relaxin-3 projections to mid- and fore-brain regions containing neurons expressing relaxin-family peptide receptor 3 (RXFP3) (Ma et al., 2007; Smith et al., 2010).

RXFP3 is the cognate receptor for relaxin-3 (Liu et al., 2003) and triggers $G_{i/o}$-protein-mediated inhibition of cyclic adenosine monophosphate (cAMP) production in response to relaxin-3 binding *in vitro* (Liu et al., 2003; Van der Westhuizen et al., 2005). Similarly, electrophysiological studies of RXFP3 activation in brain slices typically identified membrane hyperpolarisation and neuronal inhibition (Blasiak et al., 2013; Kania et al., 2017; Ch'ng et al., 2019). As such, relaxin-3 signalling, likely working in conjunction with co-expressed, fast-acting GABA neurotransmission (Ma et al., 2007), appears to promote arousal, in part through the selective disinhibition of key neural networks (Ma et al., 2018). One such network, the septohippocampal pathway, contains inhibitory, parvalbumin-positive medial septal neurons and hippocampal somatostatin- and parvalbumin-positive interneurons that express RXFP3 in rat and mouse brain (Haidar et al., 2017; Albert-Gasco et al., 2018a; Rytova et al., 2019; Haidar et al., 2019). Selective blockade or deletion of RXFP3 (Ma et al., 2009a; Haidar et al., 2017, 2019) in these regions impairs spatial memory and associated hippocampal theta rhythm, to which relaxin-3 NI neurons are strongly phase-locked (Ma et al., 2013). Social recognition is also influenced by relaxin-3 signalling, as RXFP3 agonists, delivered by viral vector-mediated expression in ventral hippocampus (Rytova et al., 2019) or intracerebroventricular infusion (Albert-Gasco et al., 2018b), reduce interactions of rats with novel conspecifics.

Additional pharmacological studies targeting RXFP3 have shown effects on interrelated anxiety (Ryan et al., 2013; Zhang et al., 2015), feeding (McGowan et al., 2006; Shabanpoor et al., 2012) and motivated (Smith et al., 2014a) behaviours, most likely via actions within limbic and hypothalamic networks (Kania et al., 2017). A key role for this system in innate anxiety is also highlighted by independent relaxin-3 and RXFP3 gene knock-out mouse lines, which display a small, but consistent, decrease in anxiety behaviour (Watanabe et al., 2011; Hosken et al., 2015). Considering these and other described functions, in addition to its discrete expression profile and neuromodulatory nature, the relaxin-3/RXFP3 system offers considerable potential as a therapeutic target (see Smith et al., 2014b; Kumar et al., 2017; Ma et al., 2017b for review). In advancing our understanding of relaxin-3 neural circuitry, which to date has largely relied on pharmacological and gene knock-out models, we sought to take advantage of modern transgenic approaches. Recent chemo- (Ma et al., 2017a) and opto-genetic (Szonyi et al., 2019) manipulations have provided powerful insights into the ability of NI neurons to fine-tune behavioural responses and memory formation. Our laboratory has also established adeno-associated viral (AAV) vectors for efficient transgene delivery into NI neurons (Callander et al., 2012; Ma et al., 2017a). However, these experiments targeted either GABAergic NI neurons or the entire nucleus, thus affecting multiple populations, including but not limited to, relaxin-3 neurons (Ma et al., 2007; Ma and Gundlach, 2015).

The present study therefore aimed to identify a promoter sequence capable of selectively driving transgene expression in relaxin-3 NI neurons following viral vector transduction. Tanaka et al. (2009) are, to our knowledge, the only other investigators to describe a relaxin-3 promoter. Their experiments reported promoter activity from a 1.8 kilobase (kb) sequence, located directly 5′ of the mouse relaxin-3 gene, which was upregulated following stimulation of the CRF_1 receptor and downstream cAMP-protein kinase A (PKA) pathway. Although these experiments demonstrated this sequence could drive enhanced green fluorescent protein (EGFP) expression in cultured neuroblastoma cells expressing relaxin-3, they did not determine the cell-type specificity of the observed promoter activity. As such, we assessed the ability of an approximately analogous 1736 base pair (bp) region of rat genomic DNA to provide cell-type specific transduction of relaxin-3 NI neurons.

In addition, we have discovered that tropomyosin receptor kinase A (TrkA), a high-affinity receptor for nerve-growth factor (NGF), is exclusively co-expressed with relaxin-3 in rat NI neurons (see e.g. Sobreviela et al., 1994 and Results). In light of existing evidence for cell-type specific activity from human or mouse TrkA promoter and enhancer elements in neuroblastoma cell lines (Chang et al., 1998; Sacristan et al., 1999) and mouse trigeminal and dorsal root ganglia during development (Ma et al., 2000), we also attempted to achieve targeted AAV transduction of relaxin-3 neurons in rat NI using an 880 bp TrkA promoter sequence.

In contrast to previous data obtained using different experimental conditions, we observed widespread non-specific transduction of neurons in the rat NI and neighbouring dorsal tegmental nuclei, following stereotaxic injection of an AAV vector expressing mCherry using the 880 bp TrkA promoter. However, a similar AAV vector, engineered to express mCherry under the control of the 1736 bp rat relaxin-3 promoter, was able to transduce relaxin-3 NI neurons with 98% specificity for at least eight weeks following transgene delivery.

Experimental procedures

Animals

All experiments were approved by The Florey Institute of Neuroscience and Mental Health Animal Ethics Committee and conducted in accordance with ethical guidelines provided by the National Health and Medical Research Council of Australia. Sprague-Dawley rats (250–300 g males, Animal Resources Centre, Canning Vale, WA, Australia) were single-housed with free access to water and standard chow under ambient conditions (21 °C) and a 12 h light:dark cycle (lights on 07:00). Every effort was made to minimize the number of rats used and any stress resulting from the procedures described.

Relaxin-3 and TrkA promoter design

Pairwise alignments of rat genomic sequences (Jul. 2014 (RGSC 6.0/rn6) assembly) (Havlak et al., 2004; Gibbs et al., 2004) with other vertebrate genomes, including mouse (Dec. 2011 (GRCm38/mm10) assembly) (Mouse Genome Sequencing Consortium et al., 2002) and human (Dec. 2011 (GRCh38/hg38) assembly) (Lander et al., 2001), were visualised using the UCSC Genome Browser's chain track feature (Kent et al., 2002). Based on the location of two regions upstream of the relaxin-3 gene, conserved in rodents but not primates, we initially attempted to isolate a 3.5 kb sequence from rat genomic DNA using polymerase chain reaction (PCR). However, 1.8 kb of poorly conserved DNA between these regions was skipped during PCR amplification (Supplementary Fig. 1A), resulting in a 1736 bp relaxin-3 promoter amplicon. Given that the conserved regions of interest were retained, we proceeded to characterise this 1736 bp sequence. Similar genomic comparisons using the UCSC Genome Browser were performed for the TrkA promoter region, revealing a high degree of sequence conservation in the non-coding region between the closely adjacent TrkA and insulin receptor-related protein (INSRR) genes (Supplementary Fig. 1B). Additional consideration was given to incorporate regions of rat genome analogous to minimal promoter and enhancer elements described for mouse (Sacristan et al., 1999; Ma et al., 2000) and human (Chang et al., 1998), resulting in selection of an 880 bp TrkA promoter region for characterisation (synthesised by GenScript (Piscataway, NJ, USA)). Data presented in Supplementary Fig. 1 were adapted from BLAT searches (Kent, 2002) of each promoter against the rat genome (Jul. 2014 (RGSC 6.0/rn6) assembly) in the UCSC Genome Browser.

Generation of plasmid vectors

Plasmids containing recombinant AAV vector genomes, with mCherry as a marker for promoter activity, were prepared using the

Gateway cloning system, as described by White et al. (2011). To facilitate this, a Gateway-compatible AAV backbone plasmid (pAM-Gateway) was created using SpeI and HindIII cut sites to replace CAG promoter and EGFP coding sequences of pAM-DCA-EcoRI-EGFP (Callander et al., 2012) with an attR1-R2 cloning cassette. The 1736 bp rat relaxin-3 promoter sequence was cloned using forward (5′-attB1-CCTGCAAACTTGTCTGTGTAC-3′) and reverse (5′-attB5r-CAGCTGAGA TGCCTGCGA-3′) primers. Additional forward (5′-attB1-GAACGGTTCC CAGCTCACACGTCCG-3′) and reverse (5′-attB5r-CGCGGCGGCGCCCGC CTAG-3′) primers were used to amplify the 880 bp rat TrkA promoter sequence. pENTR-L1-Rln3-R5 and pENTR-L1-TrkA-R5 plasmids were created by recombination of respective PCR products (50 fmol) with pDONR-P1-P5r. Further recombination steps, involving 10 fmol of either pENTR-L1-Rln3-R5 or pENTR-L1-TrkA-R5, with 10 fmol pENTR-L5-mCherry-L2 and 20 fmol of pAM-Gateway destination vector, produced pAM-Rln3-mCherry and pAM-TrkA-mCherry plasmids. Each recombination reaction used Clonase™II reagents (Life Technologies, Mulgrave, VIC, Australia) and was incubated at 25 °C for 16 h. pDONR-P1-P5r, pENTR-L5-mCherry-L2 and plasmid containing attR1-R2 cloning cassette, used in generating pAM-Gateway, were a gift from Dr Melanie White (A*STAR, Singapore). Constructs containing PCR amplified promoter inserts were verified by Sanger sequencing (Australian Genome Research Facility, Melbourne, VIC, Australia).

AAV vector production and titration

Mosaic serotype 1/2 AAV vectors were produced as described (Zolotukhin et al., 1999; Ganella et al., 2013). In brief, genomes from pAM-TrkA-mCherry or pAM-Rln3-mCherry were packaged into AAV1/2 capsids by co-transfection into HEK293FT cells with pDPI and pDPII plasmids (Grimm et al., 2003). Harvested vectors were purified by iodixanol gradient centrifugation and the titre, reported as genomic copies (gc) per ml, was determined using quantitative PCR with primers against the woodchuck hepatitis virus post-transcriptional regulatory element (WPRE) sequence, as described (Ma et al., 2017a).

Stereotaxic injection of colchicine or AAV vectors

Rats were placed in an enclosed chamber and anaesthesia induced by inhalation of 4% isoflurane before transfer to a stereotaxic frame (Kopf Instruments, Tujunga, CA, USA). Anaesthesia was maintained during surgical procedures with 2–3% isoflurane in air, delivered via a rat anaesthetic mask at 200 ml/min. Depth of anaesthesia was verified regularly by lack of eye-blink reflex in response to medial canthus touch and lack of withdrawal response to firm hind paw pinch. Body temperature was maintained throughout surgery with a heat pad. Rats were administered meloxicam intraperitoneally (1.5 mg/kg; Boehringer-Ingelheim, St Joseph, MO, USA), and bupivacaine subcutaneously at the top of the scalp (0.5% in sterile water), prior to an incision to expose the skull surface. A burr hole was drilled through the skull based on stereotaxic coordinates (Paxinos and Watson, 2014) as detailed below.

In studies to maximise the level of peptide and protein accumulation in the soma of NI neurons for the comparative immunohistochemical detection of relaxin-3 and TrkA, a cohort of rats (n = 5) were treated with intracerebroventricular colchicine. An injector needle (29 G) attached to polyethylene tubing connected to a 10 μl Hamilton syringe (Harvard Apparatus, Holliston, MA, USA) mounted on an infusion pump (11-Plus, Harvard Apparatus) was used to deliver colchicine (80 μg in 5 μl sterile saline) at a rate of 1 μl/min to the right lateral cerebral ventricle (AP -0.2 mm, ML + 1.5 mm, DV -4 mm from bregma). To minimise reflux of injectate up the cannula, the needle was left in place for 10 min and then withdrawn.

In separate cohorts of rats, promoter activity was characterised by stereotaxic injection of AAV vectors into NI. Prior to injection, AAV1/2-Rln3-mCherry (1.86 × 10^{11} gc/ml) or AAV1/2-TrkA-mCherry (2.04 × 10^{11} gc/ml) was mixed with an AAV1/2-CAG-EGFP vector (as

described by Callander et al., 2012; 9.08 × 10^{10} gc/ml), to allow visualisation of total viral vector spread from the injection site, as reflected by EGFP expression driven by the non-specific CAG promoter. These values reflect the final titre of each vector when injected and account for dilution caused by mixing. Rats (n = 3 per group) received 0.4 μl bilateral injections of one of these viral vector mixtures, delivered into the NI at 0.1 μl/min using a pulled glass pipette attached to a 1 μl syringe. The coordinates used for injections were: AP -2.5 mm; ML ± 0.1 mm; DV -6.5 mm from lambda; incisor bar -12.5 mm. To minimise reflux, the pipette was left in place for 10 min after each injection, raised 1 mm and held in place for a further one min, before being slowly withdrawn.

Following colchicine or viral vector delivery, the incision was sutured, swabbed with providone iodine, and rats regained consciousness in a warm chamber. Rats were euthanised 24 h following colchicine infusion, whereas those that received viral vector injections were treated with meloxicam for a further 2 d following surgery, and maintained for 8 wk prior to sacrifice.

Histology and immunostaining

Rats were euthanised by intraperitoneal injection of pentobarbitone (100 mg/kg) before transcardial perfusion with 300 ml of ice-cold phosphate-buffered saline (PBS, 0.1 M, pH 7.4) followed by 400 ml of 4% paraformaldehyde in PBS (PFA). Dissected brains were fixed in ice-cold 4% PFA for a further 1–2 h before undergoing cryoprotection by submersion in a 30% sucrose/PBS solution at 4 °C for 3 d.

For immunostaining and assessment of viral vector transduction in NI, coronal sections (40 μm) from bregma -10.4 mm to -8.4 mm (Paxinos and Watson, 2014) were collected free-floating in PBS. Sections were transferred to blocking buffer (10% v/v normal horse serum (NHS) in PBS with 0.1% Triton-X) and incubated for 1 h at room temperature with agitation. NHS blocked sections from colchicine-treated rats were incubated in PBS containing mouse anti-relaxin-3 (1:5; HK4-144-10 (Kizawa et al., 2003; Tanaka et al., 2005; Ma et al., 2007)) and rabbit anti-TrkA (1:10,000; kindly provided by Dr Louis Reichardt, UCSF, CA, USA; (Clary et al., 1994; Sobreviela et al., 1994; Holtzman et al., 1995)) antibodies with 2% NHS and 0.1% Triton-X at 4 °C for 72 h. Some sections were incubated with *only* the mouse anti-relaxin-3 antiserum or the rabbit anti-TrkA antisera to check for non-specific interactions in the double-label studies. Coronal NI sections from rats that received AAV vector injections were incubated in PBS containing mouse anti-relaxin-3 (1:5; HK4-144-10) and rabbit anti-red fluorescent protein (1:1000; Rockland Immunochemicals, Limerick, PA, USA) antibodies with 2% NHS and 0.1% Triton-X for 24 h at 4 °C.

Sections were washed 3 × 10 min in PBS following primary antibody incubations. Sections were incubated in PBS containing Alexa Fluor-594-conjugated donkey anti-rabbit and Alexa Fluor-647-conjugated donkey anti-mouse antibodies (1:500 each; Jackson ImmunoResearch, West Grove, PA, USA) as well as bis-benzimide H (Hoechst) 33,342 (1 μg/ml; Sigma-Aldrich, Castle Hill, NSW, Australia) for 1 h at room temperature. Sections were washed 3 × 5 min in PBS, slide-mounted and coverslipped with Dako fluorescence mounting medium (Agilent Technologies, Santa Clara, CA, USA).

In studies to visualise NI-transduced neuronal projections in the medial septum (MS), 40 μm coronal sections from bregma +1.56 mm to 0.00 mm were collected and blocked with NHS as described. Following incubation in PBS containing 1:500 mouse anti-mCherry (Developmental Studies Hybridoma Bank, University of Iowa, Iowa City, IA, USA) and 1:500 rabbit anti-GABA (Sigma-Aldrich) antibodies, with 2% NHS, 0.1% Triton-X and 0.5% thimerosal (Sigma-Aldrich) for 72 h at room temperature, sections were washed 3 × 10 min in PBS. A further 2 h incubation at room temperature in PBS solution containing 1:500 Alexa-594-conjugated donkey anti-mouse and Alexa-647 conjugated donkey anti-rabbit antibodies (Jackson ImmunoResearch) as well as bis-benzimide H (Hoechst) 33342 (1 μg/ml) preceded

3 × 5 min washes in PBS and slide-mounting as described.

Imaging and quantitative analysis

An LSM 780 Zeiss Axio Imager 2 laser scanning confocal microscope (Carl Zeiss AG, Oberkochen, Germany) was used to acquire images. To assess promoter activity in NI neurons, relaxin-3-immunoreactivity (IR) (Alexa Fluor-647) and mCherry-IR (Alexa Fluor-594), as well as Hoechst nuclear stain (to assist with cell counting) and innate EGFP, were imaged using a 20× air objective lens in every third section from bregma -9.00 mm to -9.84 mm for each rat. Centred on the midline directly ventral to the fourth ventricle, 1.57 mm × 1.19 mm images were collected using a stitching stage and Zen Black software (Carl Zeiss AG). Planes were collected at 3 µm intervals through the z-axis and used to produce maximum projection images in Fiji software (Schindelin et al., 2012), where manual cell counts and colocalisation analysis of fluorescent soma were also performed. Percentages calculated for the specificity and efficiency of viral vector transduction (see Results for further descriptions) are reported as mean ± standard error of the mean (SEM). High magnification images of relaxin-3-IR (Alexa Fluor-647) and TrkA-IR (Alexa Fluor-594) in NI, or mCherry-IR (Alexa Fluor-594), GABA-IR (Alexa Fluor-627), innate EGFP and Hoechst nuclear stain in MS, were collected using a 63× oil immersion objective lens, with images collected at 2 µm intervals through the z-axis. All microscopy data in figures presented are maximum intensity z-stack projections.

Results

Established and emerging transgenic techniques offer powerful approaches to understanding neural circuit structure and function. Such techniques have been applied in recent molecular and behavioural studies utlising viral vector injections for targeted NI expression in wild-type or transgenic rodents (Ma et al., 2017a; Szonyi et al., 2019). However, these experiments affected multiple, heterogenous populations of NI neurons (Ma et al., 2007; Ma and Gundlach, 2015), highlighting the need for more selective methods of transgene expression. In the present study, we sought to identify a promoter sequence capable of selectively driving transgene expression in relaxin-3 NI neurons following AAV vector transduction. In addition to a conserved region upstream of the rat relaxin-3 gene coding sequence, we also characterised the activity of a promoter region for the TrkA receptor, which is selectively co-expressed with relaxin-3 in NI neurons. The promoter activity of each sequence, as reflected by mCherry expression in transduced neurons, was characterised against immunolabelling for the relaxin-3 peptide. Co-injection of a separate, EGFP-expressing vector allowed relaxin-3 and TrkA promoter activity to be compared with the constitutive CAG promoter, while also facilitating visualisation of AAV vector spread outside the NI.

Targeted transduction of rat relaxin-3 NI neurons using a novel relaxin-3 promoter

In these studies, data were collected from rats (n = 3) displaying neuronal transduction by AAV1/2-Rln3-mCherry and AAV1/2-CAG-EGFP (Fig. 1A) distributed bilaterally throughout the NI (Fig. 1B-E), with data excluded from rats in which off-target or limited spread of transduction was observed (Fig. 1F). Neurons displaying fluorescence in individual optical wavelength channels for EGFP, mCherry-IR or relaxin-3-IR were counted, with further counts of neurons containing EGFP and/or mCherry-IR in addition to relaxin-3-IR also performed (Supplementary Table 1). The specificity (proportion of transduced cells expressing relaxin-3) and efficiency (proportion of total relaxin-3 population transduced) of each promoter was calculated from these cell counts (Supplementary Table 2, Fig. 1G). Similar transduction efficiencies were observed between AAV1/2-Rln3-mCherry and AAV1/2-

CAG-EGFP vectors, with a majority of relaxin-3-IR NI neurons displaying EGFP (73 ± 8%) and/or mCherry-IR (70 ± 2%) fluorescence. As expected, non-specific transduction by AAV1/2-CAG-EGFP was evident throughout the NI and in regions of some neighbouring nuclei (e.g. DTg, Fig. 1B), leading to relaxin-3-IR detection in only 30 ± 5% of EGFP expressing neurons. Importantly, this viral vector spread outside the NI was only reflected by CAG promoter-driven EGFP expression, with mCherry expression under the control of the Rln3 promoter limited to the NI (Fig. 1F). Of the total number of neurons transduced by AAV1/2-Rln3-mCherry, virtually all (98 ± 1%) were found to contain relaxin-3-IR (Fig. 1G). This was despite non-specific transduction of closely adjacent NI neurons by AAV1/2-CAG-EGFP (Fig. 1C-E), indicating that the targeted mCherry expression was dependent on promoter activity rather than viral vector tropism.

AAV1/2-Rln3-mCherry transduction identifies direct NI relaxin-3 neuron input to GABAergic medial septum circuitry

Multiplex *in situ* hybridisation studies have shown that *Rxfp3* mRNA is strongly co-expressed with vesicular GABA transporter (*vGAT*) mRNA in MS neurons (Albert-Gasco et al., 2018a; Haidar et al., 2019). In studies to build on these findings and demonstrate the utility of AAV1/2-Rln3-mCherry in mapping networks formed by relaxin-3 NI neurons, we labelled coronal sections through the MS of rats used in the analysis of promoter specificity for GABA- and mCherry-IR (n = 2 rats; Fig. 2). Staining of MS sections for relaxin-3 was not undertaken, given the exclusive expression of mCherry in relaxin-3 NI neurons observed. Large fibres containing EGFP emanating from neurons transduced by the control AAV1/2-CAG-EGFP vector were densely concentrated in the medial septum/diagonal band complex (MS/DB; Fig. 2A), consistent with neural tract-tracing studies of NI (Goto et al., 2001; Olucha-Bordonau et al., 2003; Ma et al., 2009a); confirming that ascending efferent projections from the NI pass through and/or terminate in the MS/DB. In a subset of these MS/DB EGFP fibres, red fluorescence resulting from AAV1/2-Rln3-mCherry transduced NI neurons was also present (Fig. 2C), confirming relaxin-3 NI neurons send direct projections to the MS/DB. High-magnification confocal images in MS also revealed fine structures containing EGFP and mCherry-IR fluorescence, indicative of potential axon terminals or boutons (Fig. 2B-D). Of particular note, given existing evidence for RXFP3 mRNA expression by vGAT mRNA-positive MS neurons, many of the putative relaxin-3 NI (mCherry-positive) nerve terminals were observed in close apposition to MS neurons containing GABA-IR (Fig. 2C).

TrkA is co-expressed with relaxin-3 in rat NI neurons

In parallel to studies characterising the relaxin-3 promoter, we investigated whether a TrkA promoter sequence could be used for targeted transduction of relaxin-3 neurons. Dense immunostaining of TrkA has previously been detected in the clearly distinguishable neurons that comprise the rat NI, despite the fact that this anatomical structure was incorrectly identified as the *prepositus hypoglossal nucleus* in that report (see Fig. 11, (Sobreviela et al., 1994)). The *prepositus hypoglossal nucleus* also expresses dense TrkA mRNA and immunoreactivity (Gibbs and Pfaff, 1994; Sobreviela et al., 1994), but it is clearly distinct and distinguishable from the NI. In extending and clarifying these earlier studies, we performed dual immunohistochemistry for TrkA and relaxin-3 to assess their degree of co-expression in NI neurons (n = 5 rats). As expected, immunofluorescence detection revealed TrkA immunoreactive neurons throughout the NI (Fig. 3B) and most, if not all, of these neurons also displayed relaxin-3 immunofluorescence (Fig. 3A,C). Furthermore, an overlay of TrkA and relaxin-3 immunofluorescence staining in separate, adjacent sections revealed an identical neuronal co-distribution, despite some differences in the subcellular distribution of the immunoreactive materials (Fig. 3D-F). This co-expression is consistent with identified roles for NGF/TrkA
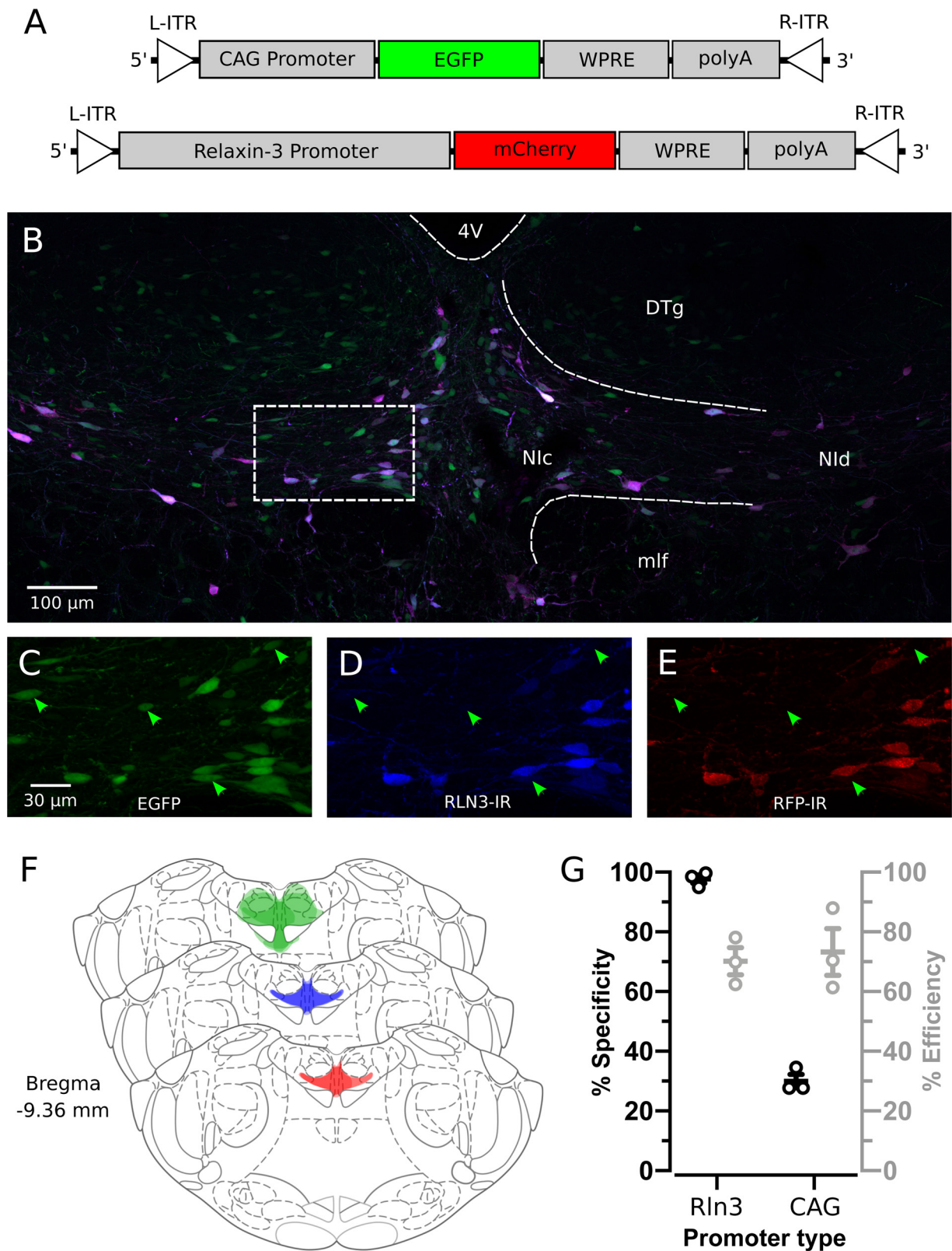
(caption on next page)

signalling in supporting the survival and function of key projection-neuron networks, such as cholinergic basal forebrain and GABAergic septohippocampal systems (Rocamora et al., 1996; Conner et al., 2009), and provided the basis for studies of TrkA promoter specificity in rat NI.

TrkA promoter drives non-specific transgene expression in dorsal pons of adult rats

As described for rats receiving AAV1/2-Rln3-mCherry injections, inclusion of data from rats co-injected with AAV1/2-TrkA-mCherry and

Fig. 1. *Neuronal transduction by AAV1/2-Rln3-mCherry*. **(A)** Schematic design of recombinant AAV genomes for AAV1/2-CAG-EGFP and AAV1/2-Rln3-mCherry vectors (*L-ITR*, left inverted terminal repeat; *WPRE*, woodchuck hepatitis virus post-transcriptional regulatory element; *polyA*, SV40 poly A sequence; *R-ITR*, right inverted terminal repeat). **(B)** Representative image of innate fluorescence produced by EGFP (green) and fluorescence produced by mCherry (red) and relaxin-3 (blue) immunoreactivity, eight weeks after stereotaxic injection of AAV1/2-CAG-EGFP and AAV1/2-Rln3-mCherry vectors targeting NI (*4V*, fourth ventricle; *DTg*, dorsal tegmental nucleus; *mlf*, medial longitudinal fasciculus; *NIc*, NI *pars compacta*; *NId*, NI *pars dissipata*). **(C–E)** Individual fluorescence channels from **(B)** are illustrated at higher magnification. Transduced neurons lacking relaxin-3 immunoreactivity (RLN3-IR) are indicated by green arrowheads (i.e., AAV1/2-CAG-EGFP transduced only). Note there are no AAV1/2-Rln3-mCherry-transduced neurons in the field that do not contain RLN3-IR) (*RFP-IR*, red fluorescent protein (mCherry) immunoreactivity). **(F)** Distribution of neurons transduced by AAV1/2-CAG-EGFP (green) or AAV1/2-Rln3-mCherry (red) vectors, with RLN3-IR (blue) at bregma -9.36 mm in the rats (n = 3) used in the analysis. **(G)** Quantification of promoter specificity (proportion of transduced neurons containing RLN3-IR (black circles)) and efficiency (proportion of total RLN3-IR neurons transduced (grey circles)). Data points for each variable represent individual rats (n = 3) and bars represent mean ± SEM.

AAV1/2-CAG-EGFP in the final analyses (Fig. 4, n = 3) was dependent on successful bilateral transduction by these vectors throughout the NI. No significant difference was observed in the efficiency of relaxin-3 NI neuronal transduction by AAV1/2-CAG-EGFP in these rats (63 ± 6%; P = 0.33 (Student's t-test)) compared to the Rln3 promoter cohort. However, due to some variation in spread of injected vectors to regions surrounding the NI, the calculated specificity for AAV1/2-CAG-EGFP in this group (18 ± 1%, Fig. 4G) was slightly lower. A similar distribution of non-specifically transduced neurons in NI and adjacent regions was observed for AAV1/2-TrkA-mCherry (Fig. 4B, F), resulting in only 11 ± 1% of mCherry-IR neurons containing relaxin-3-IR. Differences in TrkA and CAG promoter activity within the NI (Fig. 4C-E) resulted in a relatively low calculated efficiency as well, with AAV1/2-TrkA-mCherry transducing around one-third (32 ± 8%) of relaxin-3-IR NI neurons. Additional TrkA immunolabelling (data not shown) confirmed widespread transduction of neurons lacking TrkA immunoreactivity by AAV1/2-TrkA-mCherry in these rats.

Discussion

Ascending relaxin-3 neurons form abundant connections with key mid- and fore-brain targets. In the rat, these connections are likely maintained by retrograde NGF signalling via TrkA (Harrington and Ginty, 2013), in light of the observed selective expression of TrkA with relaxin-3. Previous reports of cell-type specific transgene expression using TrkA promoter elements in other species and contexts (Chang et al., 1998; Sacristan et al., 1999; Ma et al., 2000) suggested this approach could allow targeted viral vector transduction of rat TrkA/relaxin-3 NI neurons. However, an AAV vector engineered to express mCherry under the control of an 880 bp TrkA promoter sequence failed to provide cell-type specific expression in rat NI. In contrast, using a previously uncharacterised 1736 bp relaxin-3 promoter sequence, we were able to efficiently transduce relaxin-3 NI neurons with 98% specificity.

Several technical obstacles must be overcome to successfully use promoter sequences to achieve cell-type specific transgene expression from a viral vector. Viral vectors have a limited packaging capacity, with AAV vectors failing to incorporate recombinant genomes larger than ~4.7 kb (Wu et al., 2010). Feasible promoter candidates must therefore be restricted to several kilobases or less, depending on the vector used. As a result, loss of regulatory elements such as histone binding sites, located potentially tens of kilobases upstream from the gene coding sequence of interest, can be a major impediment to this experimental approach. Cell-type specific promoters also need to be able to suppress expression driven by the AAV inverted terminal repeat (ITR) sequences. These ITRs, which are essential for AAV genome packaging, can drive transgene expression independently of other promoter elements (Flotte et al., 1993). Furthermore, high viral vector
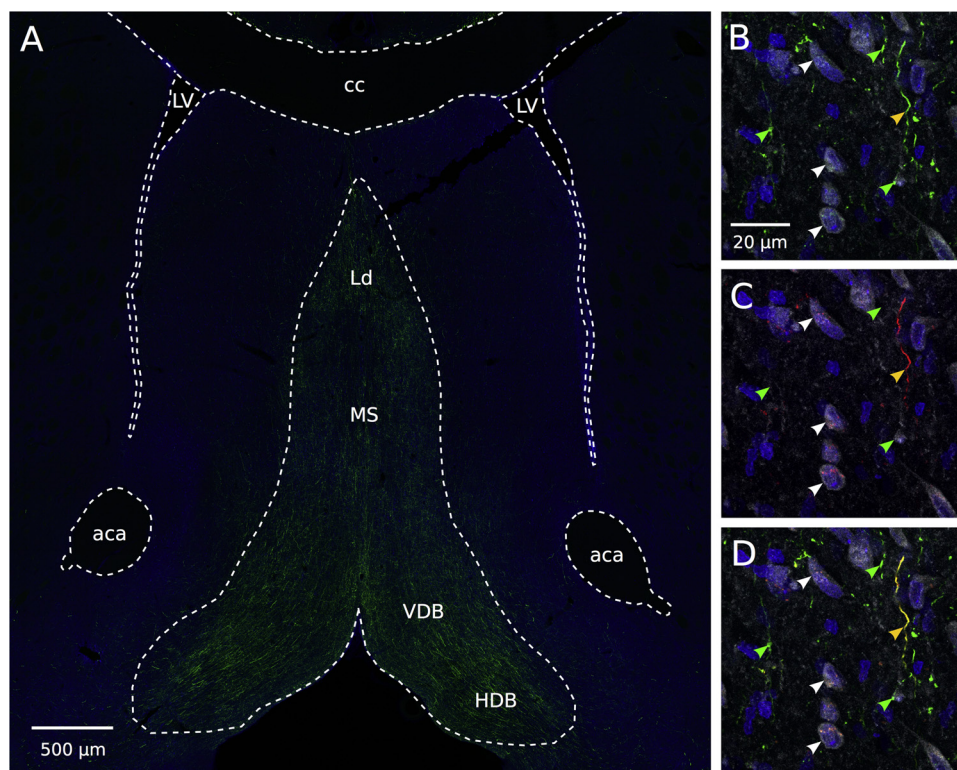

Fig. 2. *Visualisation of AAV1/2-Rln3-mCherry transduced NI projections, with close apposition to GABAergic neuronal soma in the medial septum.* Fluorescent protein expression was visualised in efferent fibres projecting from transduced NI neurons to the medial septum/diagonal band complex (MS/DB) of rats which received AAV1/2-Rln3-mCherry and AAV1/2-CAG-EGFP injections ((A); EGFP, *green*; mCherry-IR, *red*; Hoechst nuclear stain, *blue*; representative image from n = 2 rats). **(B–D)** In addition to larger fibres passing through the MS which contained both mCherry-IR and EGFP (yellow arrowhead), or EGFP alone (green arrowheads), fine processes and potential terminals from transduced NI neurons were observed in close apposition to neuronal soma containing GABA-IR (*white*; putative contacts indicated by white arrowheads). Representative images of merged **(D)** or separate non-specific EGFP **(B)** and relaxin-3 promoter dirven mCherry-IR **(C)** channels highlight the ability of this approach to provide targeted mapping of fibres and terminals projecting from transduced relaxin-3 NI neurons. Abbreviations: *aca*, anterior commissure, anterior part; *cc*, corpus callosum; *HDB*, nucleus of the horizontal limb of the diagonal band; *IR*, immunoreactivity; *Ld*, lambdoid septal zone; *LV*, lateral ventricle; *MS*, medial septum; *VDB*, nucleus of the vertical limb of the diagonal band.
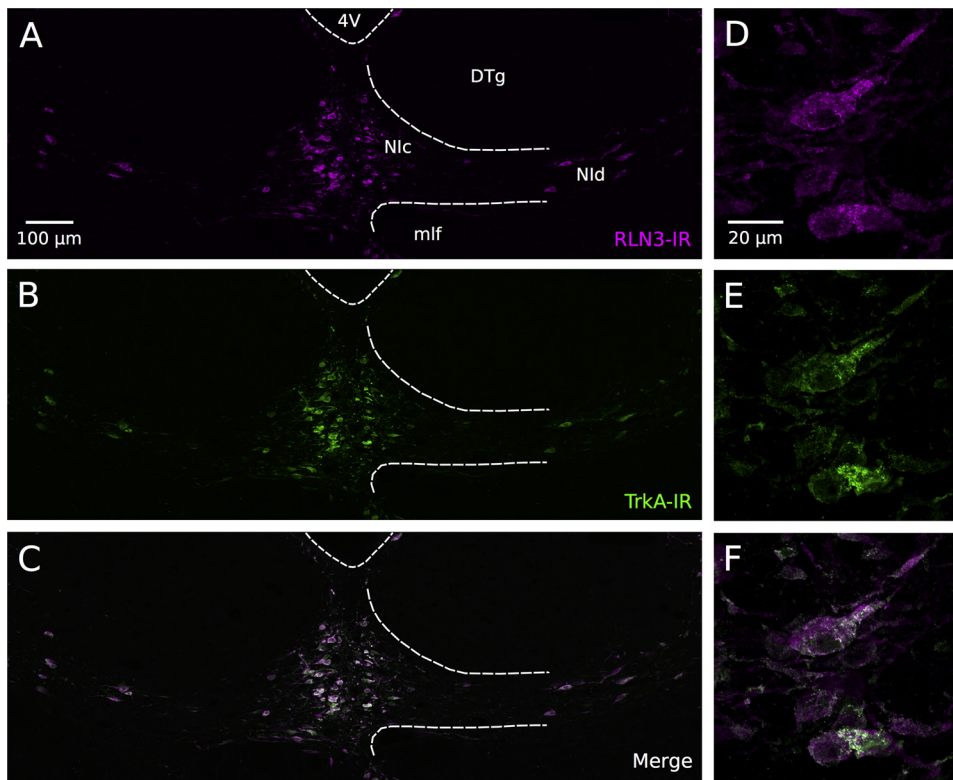
Fig. 3. *Co-expression of relaxin-3 and TrkA immunoreactivity in rat NI*. Overview of immunofluorescence for relaxin-3 (RLN3) (**A**, magenta) and TrkA (**B**, green) in the NI, with a merged image revealing the strong co-expression and resultant overlap of channels (**C**, white). High magnification images of individual (**D**, **E**) and merged (**F**) relaxin-3 and TrkA immunoreactivity show differences in the subcellular distribution of these co-expressed gene products in NI neurons. Abbreviations: *4V*, fourth ventricle; *DTg*, dorsal tegmental nucleus; *IR*, immunoreactivity; *mlf*, medial longitudinal fasciculus; *NIc*, NI *pars compacta*; *NId*, NI *pars dissipata*.

titres can reduce transduction specificity by increasing the number of genomic copies introduced to a cell, thus amplifying any weak, non-specific promoter activity (Kakava-Georgiadou et al., 2019). As alternative vector titres or volumes were not tested, this is an important consideration for the use of these and similar vectors in future studies. The potential for variations in transcription factor expression and/or epigenetic modifications due to cellular environment and context is also a key consideration when validating the suitability of promoters for their intended applications.

One or more of these factors may have led to the non-specific activity observed for the 880 bp rat TrkA promoter. Previous studies have identified a minimal promoter region of ~150 bp, directly upstream of human (Chang et al., 1998) and mouse (Sacristan et al., 1999) TrkA coding sequences, which provided cell-type specific transgene expression in cultured neuroblastoma cells following transient transfection. A conserved TrkA enhancer was also shown to provide cell-type specific transgene expression from a pronuclear-injected plasmid construct, independently of the minimal promoter, in trigeminal and dorsal root ganglia of P0 mouse pups (Ma et al., 2000). Although the 880 bp rat TrkA promoter region used in our AAV1/2-TrkA-mCherry vector contained regions analogous to these human and mouse minimal promoter and mouse enhancer sequences, with 59%, 96% and 87% sequence identity, respectively, we were unable to replicate the targeted expression reported *in vitro* and in P0 mice. In addition to targeting neurons in the adult rat brainstem, rather than developing mouse ganglia or cell culture, our recombinant AAV genomes by necessity contain ITR sequences that were absent from the plasmids used in earlier studies. The incorporation of further sequence 5′ to the 880 bp promoter tested may capture elements sufficient to provide cell-type specific expression, but as mentioned, would eventually be limited by the AAV vector packaging capacity.

However, the AAV1/2-Rln3-mCherry vector, containing a 1736 bp rat relaxin-3 promoter region, provided highly targeted transduction of relaxin-3 NI neurons. Transgene expression mediated by this vector was localised to the NI, where 98% of mCherry transduced neurons also contained relaxin-3 immunoreactivity. This was despite non-specific transduction of DTg and closely adjacent, non-relaxin-3 neurons in NI by co-injected AAV1/2-CAG-EGFP, emphasising that the specificity of the AAV1/2-Rln3-mCherry vector was achieved through promoter-mediated control of transgene expression and not viral vector tropism. Notably, one outcome that was apparently due to AAV1/2 vector tropism was a consistent transduction efficiency of around 70% of relaxin-3 NI neurons (with the exception of AAV1/2-TrkA-mCherry). Although alternative approaches, such as equivalent transgenic mouse or rat lines, may increase this efficiency, a purely viral vector-based methodology offers highly flexible options in targeting particular relaxin-3 neuron populations at specific time points during the lifespan of rats or mice. In the future, it will also be of interest to investigate the use of the relaxin-3 promoter vector to study the function of the smaller and more dispersed relaxin-3 neuron populations in the pontine raphe, PAG and dorsal to substantia nigra. Detailed analysis of the neurochemistry of transduced relaxin-3 neurons and their efferent connections, as demonstrated here in the MS/DB, will be valuable in determining the implications of targeted functional studies, that extend those using constitutively active promoters (Ma et al., 2017a; Szonyi et al., 2019).

The future utility of a relaxin-3-specific promoter is wide-ranging in nature. In the current study, targeted transgene expression was validated eight weeks after viral vector injection, indicating this approach would be suitable for physiological and behavioural studies within similar, if not potentially longer, time frames. New AAV constructs designed to include the relaxin-3 promoter would be able to accommodate at least 1.6 kb of transgene coding sequence. Many transgenes commonly used in modern neuroscience, including genetically-encoded calcium indicators (around 1.3 kb; Tian et al. (2009)) and fluorescently-tagged opsins (around 1.6 kb; Boyden et al. (2005)), could readily be expressed directly from an AAV vector under this relaxin-3 promoter. An AAV1/2 capsid was used here, as we have previously established its favourable tropism towards NI neurons (Callander et al., 2012), but other vectors such as lentivirus could be explored as a means of increasing packaging capacity for transgene cargo. Additional AAV packaging space could also be gained through the use of condensed
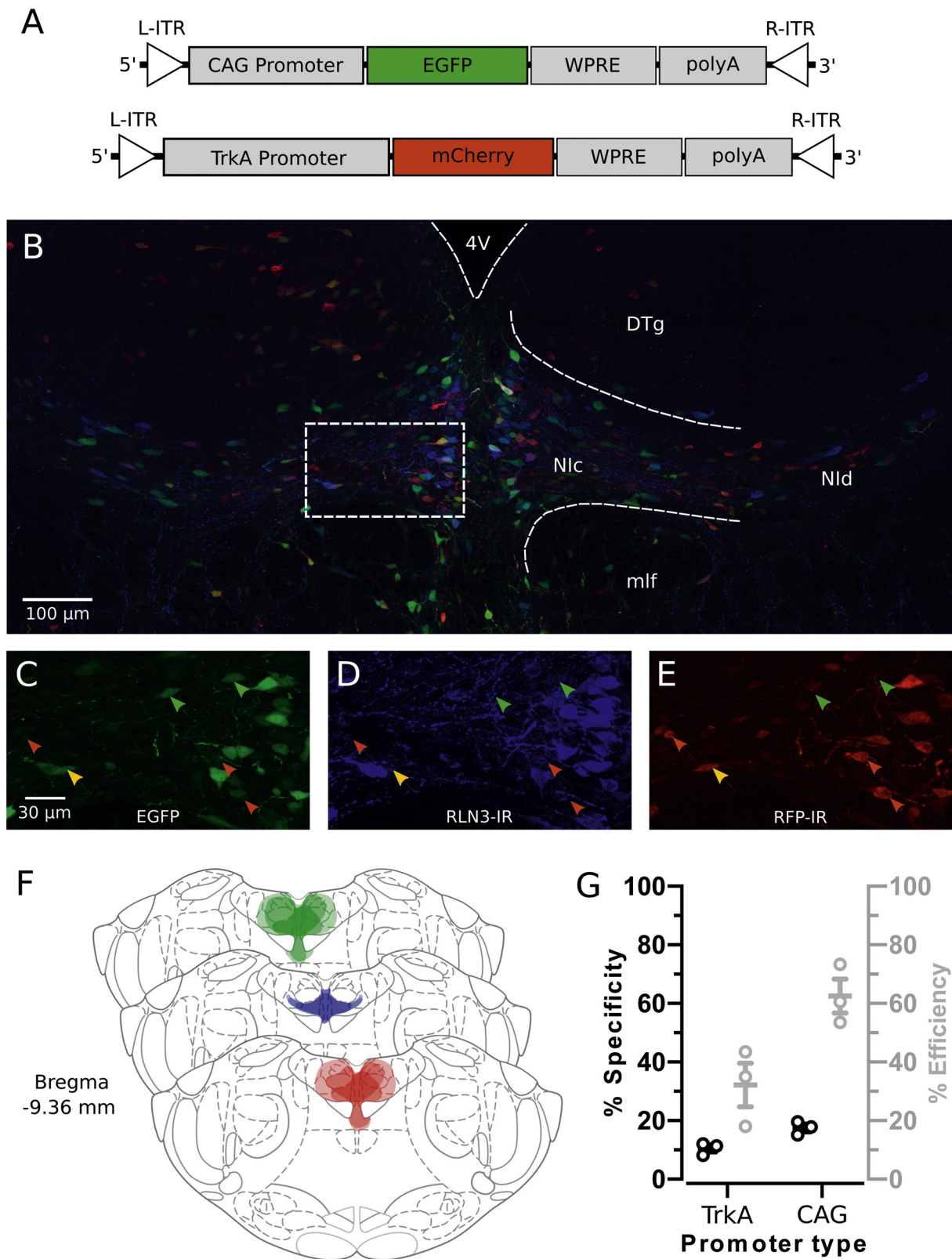
(caption on next page)

polyadenylation and posttranscriptional regulatory elements (Choi et al., 2014), and further refinement of the relaxin-3 promoter itself. Although beyond the scope of this study, determining the particular motifs that confer cell-type specificity may allow engineering of a more compact promoter, improving transgene packaging capacity as well as promoter compatibility with transcriptional amplification strategies (Liu et al., 2008). Furthermore, such endeavours could also provide insights into relaxin-3 gene regulation, similar to those reported in response to CRF signalling (Tanaka et al., 2009).

In conclusion, following transduction by an injected AAV vector

Fig. 4. *Neuronal transduction by AAV1/2-TrkA-mCherry.* **(A)** Schematic design of recombinant AAV genomes for AAV1/2-CAG-EGFP and AAV1/2-TrkA-mCherry vectors (*L-ITR*, left inverted terminal repeat; *WPRE*, woodchuck hepatitis virus post-transcriptional regulatory element; *polyA*, SV40 poly A sequence; *R-ITR*, right inverted terminal repeat). **(B)** Representative image of innate fluorescence detected from EGFP (green), together with fluorescent immunoreactivity for mCherry (red) and relaxin-3 (blue), eight weeks after stereotaxic injection of AAV1/2-CAG-EGFP and AAV1/2-TrkA-mCherry vectors targeting NI (*4V*, fourth ventricle; *DTg*, dorsal tegmental nucleus; *mlf*, medial longitudinal fasciculus; *NIc*, NI *pars compacta*; *NId*, NI *pars dissipata*). **(C–E)** Individual fluorescence channels from **(B)** illustrated at higher magnification, revealing neurons lacking relaxin-3 immunoreactivity (RLN3-IR) transduced by AAV1/2-CAG-EGFP only (green arrowheads), AAV1/2-TrkA-mCherry only (mCherry - red fluorescent protein immunoreactivity (RFP-IR); red arrowheads), and both AAV1/2-CAG-EGFP and AAV1/2-TrkA-mCherry (yellow arrowhead). **(F)** Distribution of neurons transduced by AAV1/2-CAG-EGFP (green) or AAV1/2-TrkA-mCherry (red) vectors, compared to the distribution of RLN3-IR (blue) at bregma -9.36 mm, in rats used in the analysis (n = 3). **(G)** Quantification of promoter specificity (proportion of transduced neurons containing RLN3-IR; black circles) and efficiency (proportion of total RLN3-IR neurons transduced; grey circles). Data points for each variable represent individual rats (n = 3) and bars represent mean ± SEM.

targeting the NI, we observed widespread non-specific mCherry transgene expression driven by an 880 bp TrkA promoter sequence in the adult rat brainstem. Differences in cell context, species and/or method of transgene delivery may explain discrepancies between our data and previous reports of selective expression driven from analogous promoter or enhancer regions in neuroblastoma cell lines and developing mouse nervous system. Notably, we also identified a novel cell-type specific relaxin-3 promoter, capable of transducing relaxin-3 NI neurons with 98% specificity for at least 8 weeks after AAV vector injection. Future studies utilising this promoter should lead to further insights into the molecular mechanisms that regulate relaxin-3 gene expression. Importantly, this newly characterised promoter sequence also represents a versatile tool for targeted studies of relaxin-3 circuitry in ongoing preclinical research.

Conflicts of interest

The authors have no competing interests to declare.

Acknowledgements

Appendix A. Supplementary data

Supplementary material related to this article can be found, in the online version, at doi:https://doi.org/10.1016/j.ibror.2019.11.006.

References

Albert-Gasco, H., Ma, S., Ros-Bernal, F., Sanchez-Perez, A.M., Gundlach, A.L., Olucha-Bordonau, F.E., 2018a. GABAergic neurons in the rat medial septal complex express relaxin-3 receptor (RXFP3) mRNA. Front. Neuroanat. 11, 133.

Albert-Gasco, H., Sanchez-Sarasua, S., Ma, S., Garcia-Diaz, C., Gundlach, A.L., Sanchez-Perez, A.M., Olucha-Bordonau, F.E., 2018b. Central relaxin-3 receptor (RXFP3) activation impairs social recognition and modulates ERK-phosphorylation in specific GABAergic amygdala neurons. Brain Struct. Funct. 224, 453–469.

Blasiak, A., Blasiak, T., Lewandowski, M.H., Hossain, M.A., Wade, J.D., Gundlach, A.L., 2013. Relaxin-3 innervation of the intergeniculate leaflet of the rat thalamus - neuronal tract-tracing and in vitro electrophysiological studies. Eur. J. Neurosci. 37, 1284–1294.

Blasiak, A., Siwiec, M., Grabowiecka, A., Blasiak, T., Czerw, A., Blasiak, E., Kania, A., Rajfur, Z., et al., 2015. Excitatory orexinergic innervation of rat nucleus incertus - Implications for ascending arousal, motivation and feeding control. Neuropharmacology 99, 432–447.

Boyden, E.S., Zhang, F., Bamberg, E., Nagel, G., Deisseroth, K., 2005. Millisecond-time-scale, genetically targeted optical control of neural activity. Nat. Neurosci. 8, 1263–1268.

Burazin, T.C.D., Bathgate, R.A.D., Macris, M., Layfield, S., Gundlach, A.L., Tregear, G.W., 2002. Restricted, but abundant, expression of the novel rat gene-3 (R3) relaxin in the dorsal tegmental region of brain. J. Neurochem. 82, 1553–1557.

Callander, G.E., Ma, S., Ganella, D.E., Wimmer, V.C., Gundlach, A.L., Thomas, W.G., Bathgate, R.A.D., 2012. Silencing relaxin-3 in nucleus incertus of adult rodents: a viral vector-based approach to investigate neuropeptide function. PLoS One 7, e42300.

Ch'ng, S.S., Fu, J., Brown, R.M., Smith, C.M., Hossain, M.A., McDougall, S.J., Lawrence, A.J., 2019. Characterization of the relaxin family peptide receptor 3 system in the mouse bed nucleus of the stria terminalis. J. Comp. Neurol. 527, 2615–2633.

Chang, B.B., Persengiev, S.P., de Diego, J.G., Sacristan, M.P., Zanca, D.M., Kilpatrick, D.L., 1998. Proximal promoter sequences mediate cell-specific and elevated expression of the favorable prognosis marker TrkA in human neuroblastoma cells. J. Biol. Chem. 273, 39–44.

Choi, J.H., Yu, N.K., Baek, G.C., Bakes, J., Seo, D., Nam, H.J., Baek, S.H., Lim, C.S., et al., 2014. Optimization of AAV expression cassettes to improve packaging capacity and transgene expression in neurons. Mol. Brain 7, 17.

Chronwall, B.M., Skirboll, L.R., O'Donohue, T.L., 1985. Demonstration of a pontine-hippocampal projection containing a ranatensin-like peptide. Neurosci. Lett. 53, 109–114.

Clary, D.O., Weskamp, G., Austin, L.R., Reichardt, L.F., 1994. TrkA cross-linking mimics neuronal responses to nerve growth factor. Mol. Biol. Cell 5, 549–563.

Conner, J.M., Franks, K.M., Titterness, A.K., Russell, K., Merrill, D.A., Christie, B.R., Sejnowski, T.J., Tuszynski, M.H., 2009. NGF is essential for hippocampal plasticity and learning. J. Neurosci. 29, 10883–10889.

Flotte, T.R., Afione, S.A., Solow, R., Drumm, M.L., Markakis, D., Guggino, W.B., Zeitlin, P.L., Carter, B.J., 1993. Expression of the cystic fibrosis transmembrane conductance regulator from a novel adeno-associated virus promoter. J. Biol. Chem. 268, 3781–3790.

Ganella, D.E., Callander, G.E., Ma, S., Bye, C.R., Gundlach, A.L., Bathgate, R.A.D., 2013. Modulation of feeding by chronic rAAV expression of a relaxin-3 peptide agonist in rat hypothalamus. Gene Ther. 20, 703–716.

Gibbs, R.A., Weinstock, G.M., Metzker, M.L., Muzny, D.M., Sodergren, E.J., Scherer, S., Scott, G., Steffen, D., et al., 2004. Genome sequence of the Brown Norway rat yields insights into mammalian evolution. Nature 428, 493–521.

Gibbs, R.B., Pfaff, D.W., 1994. In situ hybridization detection of trkA mRNA in brain: distribution, colocalization with p75NGFR and up-regulation by nerve growth factor. J. Comp. Neurol. 341, 324–339.

Goto, M., Swanson, L.W., Canteras, N.S., 2001. Connections of the nucleus incertus. J. Comp. Neurol. 438, 86–122.

Grimm, D., Kay, M.A., Kleinschmidt, J.A., 2003. Helper virus-free, optically controllable, and two-plasmid-based production of adeno-associated virus vectors of serotypes 1 to 6. Mol. Ther. 7, 839–850.

Haidar, M., Guevremont, G., Zhang, C., Bathgate, R.A.D., Timofeeva, E., Smith, C.M., Gundlach, A.L., 2017. Relaxin-3 inputs target hippocampal interneurons and deletion of hilar relaxin-3 receptors in 'floxed-RXFP3' mice impairs spatial memory. Hippocampus 27, 529–546.

Haidar, M., Tin, K., Zhang, C., Nategh, M., Covita, J., Wykes, A.D., Rogers, J., Gundlach, A.L., 2019. Septal GABA and glutamate neurons express RXFP3 mRNA and depletion of septal RXFP3 impaired spatial search strategy and long-term reference memory in adult mice. Front. Neuroanat. 13, 30.

Harrington, A.W., Ginty, D.D., 2013. Long-distance retrograde neurotrophic factor signalling in neurons. Nat. Rev. Neurosci. 14, 177–187.

Havlak, P., Chen, R., Durbin, K.J., Egan, A., Ren, Y., Song, X.Z., Weinstock, G.M., Gibbs, R.A., 2004. The Atlas genome assembly system. Genome Res. 14, 721–732.

Holtzman, D.M., Kilbridge, J., Li, Y.W., Cunningham, E.T., Lenn, N.J., Clary, D.O., Reichardt, L.F., Mobley, W.C., 1995. TrkA expression in the CNS - Evidence for the existence of several novel NGF-responsive CNS neurons. J. Neurosci. 15, 1567–1576.

Hosken, I.T., Sutton, S.W., Smith, C.M., Gundlach, A.L., 2015. Relaxin-3 receptor (Rxfp3) gene knockout mice display reduced running wheel activity: implications for role of relaxin-3/RXFP3 signalling in sustained arousal. Behav. Brain Res. 278, 167–175.

Jones, B.E., 2003. Arousal systems. Front. Biosci. 8, s438–451.

Kakava-Georgiadou, N., Bullich-Vilarrubias, C., Zwartkruis, M.M., Luijendijk, M.C.M., Garner, K.M., Adan, R.A.H., 2019. Considerations related to the use of short neuropeptide promoters in viral vectors targeting hypothalamic neurons. Sci. Rep. 9, 11146.

Kania, A., Gugula, A., Grabowiecka, A., de Avila, C., Blasiak, T., Rajfur, Z., Lewandowski, M.H., Hess, G., et al., 2017. Inhibition of oxytocin and vasopressin neuron activity in rat hypothalamic paraventricular nucleus by relaxin-3-RXFP3 signalling. J. Physiol. (Lond.) 595, 3425–3447.

Kastman, H.E., Blasiak, A., Walker, L., Siwiec, M., Krstew, E.V., Gundlach, A.L., Lawrence, A.J., 2016. Nucleus incertus Orexin2 receptors mediate alcohol seeking in rats. Neuropharmacology 110, 82–91.

Kent, W.J., 2002. BLAT - the BLAST-like alignment tool. Genome Res. 12, 656–664.

Kent, W.J., Sugnet, C.W., Furey, T.S., Roskin, K.M., Pringle, T.H., Zahler, A.M., Haussler, D., 2002. The human genome browser at UCSC. Genome Res. 12, 996–1006.

Kizawa, H., Nishi, K., Ishibashi, Y., Harada, M., Asano, T., Ito, Y., Suzuki, N., Hinuma, S., et al., 2003. Production of recombinant human relaxin 3 in AtT20 cells. Regul. Pept. 113, 79–84.

Kubota, Y., Inagaki, S., Shiosaka, S., Cho, H.J., Tateishi, K., Hashimura, E., Hamaoka, T., Tohyama, M., 1983. The distribution of cholecystokinin octapeptide-like structures in the lower brain stem of the rat: an immunohistochemical analysis. Neuroscience 9, 587–604.

Kumar, J.R., Rajkumar, R., Farooq, U., Lee, L.C., Tan, F.C., Dawe, G.S., 2015. Evidence of D2 receptor expression in the nucleus incertus of the rat. Physiol. Behav. 151, 525–534.

Kumar, J.R., Rajkumar, R., Jayakody, T., Marwari, S., Hong, J.M., Ma, S., Gundlach, A.L., Lai, M.K.P., et al., 2017. Relaxin' the brain: a case for targeting the nucleus incertus network and relaxin-3/RXFP3 system in neuropsychiatric disorders. Br. J. Pharmacol. 174, 1061–1076.

Kumar, J.R., Rajkumar, R., Lee, L.C., Dawe, G.S., 2016. Nucleus incertus contributes to an anxiogenic effect of buspirone in rats: involvement of 5-HT$_{1A}$ receptors. Neuropharmacology 110, 1–14.

Lander, E.S., Linton, L.M., Birren, B., Nusbaum, C., Zody, M.C., Baldwin, J., Devon, K., Dewar, K., et al., 2001. Initial sequencing and analysis of the human genome. Nature 409, 860–921.

Liu, B., Paton, J.F., Kasparov, S., 2008. Viral vectors based on bidirectional cell-specific mammalian promoters and transcriptional amplification strategy for use in vitro and in vivo. BMC Biotechnol. 8, 49.

Liu, C.L., Eriste, E., Sutton, S., Chen, J.C., Roland, B., Kuei, C., Farmer, N., Jornvall, H., et al., 2003. Identification of relaxin-3/INSL7 as an endogenous ligand for the orphan G-protein-coupled receptor GPCR135. J. Biol. Chem. 278, 50754–50764.

Ma, L., Merenmies, J., Parada, L.F., 2000. Molecular characterization of the TrkA/NGF receptor minimal enhancer reveals regulation by multiple cis elements to drive embryonic neuron expression. Development 127, 3777–3788.

Ma, S., Allocca, G., Ong-Palsson, E.K.E., Singleton, C.E., Hawkes, D., McDougall, S.J., Williams, S.J., Bathgate, R.A.D., et al., 2017a. Nucleus incertus promotes cortical desynchronization and behavioral arousal. Brain Struct. Funct. 222, 515–537.

Ma, S., Blasiak, A., Olucha-Bordonau, F.E., Verberne, A.J.M., Gundlach, A.L., 2013. Heterogeneous responses of nucleus incertus neurons to corticotrophin-releasing factor and coherent activity with hippocampal theta rhythm in the rat. J. Physiol. (Lond.) 591, 3981–4001.

Ma, S., Bonaventure, P., Ferraro, T., Shen, P.J., Burazin, T.C., Bathgate, R.A., Liu, C., Tregear, G.W., et al., 2007. Relaxin-3 in GABA projection neurons of nucleus incertus suggests widespread influence on forebrain circuits via G-protein-coupled receptor-135 in the rat. Neuroscience 144, 165–190.

Ma, S., Gundlach, A.L., 2015. Ascending control of arousal and motivation: role of nucleus incertus and its peptide neuromodulators in behavioural responses to stress. J. Neuroendocrinol. 27, 457–467.

Ma, S., Hangya, B., Leonard, C.S., Wisden, W., Gundlach, A.L., 2018. Dual-transmitter systems regulating arousal, attention, learning and memory. Neurosci. Biobehav. Rev. 85, 21–33.

Ma, S., Olucha-Bordonau, F.E., Hossain, M.A., Lin, F., Kuei, C., Liu, C.L., Wade, J.D., Sutton, S.W., et al., 2009a. Modulation of hippocampal theta oscillations and spatial memory by relaxin-3 neurons of the nucleus incertus. Learn. Mem. 16, 730–742.

Ma, S., Sang, Q., Lanciego, J.L., Gundlach, A.L., 2009b. Localization of relaxin-3 in brain of *Macaca fascicularis*: identification of a nucleus incertus in primate. J. Comp. Neurol. 517, 856–872.

Ma, S., Smith, C.M., Blasiak, A., Gundlach, A.L., 2017b. Distribution, physiology and pharmacology of relaxin-3/RXFP3 systems in brain. Br. J. Pharmacol. 174, 1034–1048.

McGowan, B.M., Stanley, S.A., Smith, K.L., Minnion, J.S., Donovan, J., Thompson, E.L., Patterson, M., Connolly, M.M., et al., 2006. Effects of acute and chronic relaxin-3 on food intake and energy expenditure in rats. Regul. Pept. 136, 72–77.

Miyamoto, Y., Watanabe, Y., Tanaka, M., 2008. Developmental expression and serotonergic regulation of relaxin 3/INSL7 in the nucleus incertus of rat brain. Regul. Pept. 145, 54–59.

Mouse Genome Sequencing Consortium, Waterston, R.H., Lindblad-Toh, K., Birney, E., Rogers, J., Abril, J.F., Agarwal, P., Agarwala, R., et al., 2002. Initial sequencing and comparative analysis of the mouse genome. Nature 420, 520–562.

Olucha-Bordonau, F.E., Teruel, V., Barcia-Gonzalez, J., Ruiz-Torner, A., Valverde-Navarro, A.A., Martinez-Soriano, F., 2003. Cytoarchitecture and efferent projections of the nucleus incertus of the rat. J. Comp. Neurol. 464, 62–97.

Paxinos, G., Carrive, P., Wang, H., Wang, P.Y., 1999. Chemoarchitectonic Atlas of the Rat Brainstem. Academic Press, San Diego, CA.

Paxinos, G., Watson, C., 2014. The Rat Brain in Stereotaxic Coordinates. Academic Press, San Diego, CA.

Rocamora, N., Pascual, M., Acsady, L., de Lecea, L., Freund, T.F., Soriano, E., 1996. Expression of NGF and NT3 mRNAs in hippocampal interneurons innervated by the GABAergic septohippocampal pathway. J. Neurosci. 16, 3991–4004.

Ryan, P.J., Buchler, E., Shabanpoor, F., Hossain, M.A., Wade, J.D., Lawrence, A.J., Gundlach, A.L., 2013. Central relaxin-3 receptor (RXFP3) activation decreases anxiety- and depressive-like behaviours in the rat. Behav. Brain Res. 244, 142–151.

Rytova, V., Ganella, D.E., Hawkes, D., Bathgate, R.A.D., Ma, S., Gundlach, A.L., 2019. Chronic activation of the relaxin-3 receptor on GABA neurons in rat ventral hippocampus promotes anxiety and social avoidance. Hippocampus 29, 905–920.

Sacristan, M.P., de Diego, J.G., Bonilla, M., Martin-Zanca, D., 1999. Molecular cloning and characterization of the 5' region of the mouse trkA proto-oncogene. Oncogene 18, 5836–5842.

Schindelin, J., Arganda-Carreras, I., Frise, E., Kaynig, V., Longair, M., Pietzsch, T., Preibisch, S., Rueden, C., et al., 2012. Fiji: an open-source platform for biological-image analysis. Nat. Methods 9, 676–682.

Shabanpoor, F., Hossain, M.A., Ryan, P.J., Belgi, A., Layfield, S., Kocan, M., Zhang, S.D., Samuel, C.S., et al., 2012. Minimization of human relaxin-3 leading to high-affinity analogues with increased selectivity for relaxin-family peptide 3 receptor (RXFP3) over RXFP1. J. Med. Chem. 55, 1671–1681.

Smith, C.M., Chua, B.E., Zhang, C., Walker, A.W., Haidar, M., Hawkes, D., Shabanpoor, F., Hossain, M.A., et al., 2014a. Central injection of relaxin-3 receptor (RXFP3) antagonist peptides reduces motivated food seeking and consumption in C57BL/6J mice. Behav. Brain Res. 268, 117–126.

Smith, C.M., Shen, P.J., Banerjee, A., Bonaventure, P., Ma, S., Bathgate, R.A.D., Sutton, S.W., Gundlach, A.L., 2010. Distribution of relaxin-3 and RXFP3 within arousal, stress, affective, and cognitive circuits of mouse brain. J. Comp. Neurol. 518, 4016–4045.

Smith, C.M., Walker, A.W., Hosken, I.T., Chua, B.E., Zhang, C., Haidar, M., Gundlach, A.L., 2014b. Relaxin-3/RXFP3 networks: an emerging target for the treatment of depression and other neuro psychiatric diseases? Front. Pharmacol. 5, 46.

Sobreviela, T., Clary, D.O., Reichardt, L.F., Brandabur, M.M., Kordower, J.H., Mufson, E.J., 1994. TrkA-immunoreactive profiles in the central nervous system: colocalization with neurons containing p75 nerve growth factor receptor, choline acetyl-transferase, and serotonin. J. Comp. Neurol. 350, 587–611.

Szonyi, A., Sos, K.E., Nyilas, R., Schlingloff, D., Domonkos, A., Takacs, V.T., Posfai, B., Hegedus, P., et al., 2019. Brainstem nucleus incertus controls contextual memory formation. Science 364 eaaw0445.

Tanaka, M., Iijima, N., Miyamoto, Y., Fukusumi, S., Itoh, Y., Ozawa, H., Ibata, Y., 2005. Neurons expressing relaxin 3/INSL 7 in the nucleus incertus respond to stress. Eur. J. Neurosci. 21, 1659–1670.

Tanaka, M., Watanabe, Y., Yoshimoto, K., 2009. Regulation of relaxin 3 gene expression via cAMP-PKA in a neuroblastoma cell line. J. Neurosci. Res. 87, 820–829.

Tian, L., Hires, S.A., Mao, T., Huber, D., Chiappe, M.E., Chalasani, S.H., Petreanu, L., Akerboom, J., et al., 2009. Imaging neural activity in worms, flies and mice with improved GCaMP calcium indicators. Nat. Methods 6, 875–881.

Van der Westhuizen, E.T., Sexton, P.M., Bathgate, R.A., Summers, R.J., 2005. Responses of GPCR135 to human gene 3 (H3) relaxin in CHO-K1 cells determined by microphysiometry. Ann. N. Y. Acad. Sci. 1041, 332–337.

Walker, L.C., Kastman, H.E., Koeleman, J.A., Smith, C.M., Perry, C.J., Krstew, E.V., Gundlach, A.L., Lawrence, A.J., 2017. Nucleus incertus corticotrophin-releasing factor 1 receptor signalling regulates alcohol seeking in rats. Addict. Biol. 22, 1641–1654.

Watanabe, Y., Tsujimura, A., Takao, K., Nishi, K., Ito, Y., Yasuhara, Y., Nakatomi, Y., Yokoyama, C., et al., 2011. Relaxin-3-deficient mice showed slight alteration in anxiety-related behavior. Front. Behav. Neurosci. 5, 50.

White, M.D., Milne, R.V.J., Nolan, M.F., 2011. A molecular toolbox for rapid generation of viral vectors to up- or down-regulate neuronal gene expression in vivo. Front. Mol. Neurosci. 4.

Wu, Z., Yang, H., Colosi, P., 2010. Effect of genome size on AAV vector packaging. Mol. Ther. 18, 80–86.

Zhang, C., Chua, B.E., Yang, A.N., Shabanpoor, F., Hossain, M.A., Wade, J.D., Rosengren, K.J., Smith, C.M., et al., 2015. Central relaxin-3 receptor (RXFP3) activation reduces elevated, but not basal, anxiety-like behaviour in C57BL/6J mice. Behav. Brain Res. 292, 125–132.

Zolotukhin, S., Byrne, B.J., Mason, E., Zolotukhin, I., Potter, M., Chesnut, K., Summerford, C., Samulski, R.J., et al., 1999. Recombinant adeno-associated virus purification using novel methods improves infectious titer and yield. Gene Ther. 6, 973–985.